2007 IEEE International Conference on
Robotics and Automation
Roma, Italy, 10-14 April 2007

A Systematic Approach to Kinematics Modeling of High Mobility Wheeled Rovers

Mahmoud Tarokh and Gregory McDermott

Department of Computer Science
San Diego State University
San Diego, CA 92182-7720, U.S.A.
tarokh@cs.sdsu.edu

***Abstract*— The paper proposes a systematic, data-driven method for kinematics modeling of high mobility wheeled rovers traversing uneven terrain. The method is based on the propagation of position and orientation velocities starting from the rover reference frame and going through various joints and linkages to the wheels. Equations of the motion are set up in a compact form, which only require the D-H parameters of the rover joints and links. To illustrate the proposed kinematics modeling, the method is applied to a rover similar to the NASA's Sample Return Rover.**

I. INTRODUCTION

Rovers with high mobility mechanisms are capable of traversing rough terrain and adapting their configurations to the changing terrain topology. They are being used increasingly in diverse applications such as terrestrial and planetary explorations [1]-[2], forestry [3], agriculture [4], mining industries [5], defense and hazardous material handling and de-mining [6]. Rovers with active suspension systems are capable of modifying and adjusting their suspension linkages and joints so as to change their center of mass thus avoiding tipover while traversing rough and inclined terrain [7]-[8].

Research efforts on kinematics modeling have been mainly limited to simple mobile robots moving on flat terrain [9]-[11]. Recently some attention has been directed towards high mobility rovers. A of study the kinematics of a particular rover is reported in [12]. A Kalman-filter approach is proposed in [13] to estimate the wheel contact angle for traction control, and [14] employs simple kinematics model and a state observer to estimate rover position/orientation velocities. In a recent paper [15], we developed a full kinematics model of an articulated rover and provided analysis of such rovers.

It is well known that a systematic and universal approach exists for kinematics modeling of robot manipulators. In this approach, a so called Denavit-Hartenberg (D-H) table is set up which specifies four parameters for forming a transformation matrix for each frame in the kinematic chain. The transformation matrices are cascaded (multiplied) to find the transformation between a base frame and a desired frame in the kinematics chain. Using the aggregate transformation matrix, the position and orientation of the desired frame are extracted. However, such a methodology does not exist for articulated rovers. The goal of this paper is to propose a systematic method, similar to those used for manipulators, for developing full kinematics models for motions over uneven terrain of general articulated high mobility wheeled rovers. The proposed approach is superior to our earlier work [15], in the sense that it is applicable to a more general class of rovers and does not require symbolic manipulation.

II. KINEMATICS MODEL DEVELOPMENT

A high mobility wheeled rover is defined as a mobile rover that consists of a main body connected to a set of wheels via a set of linkages and joints that are adjusted so as to enable it traverse uneven terrain. The joints and linkages change either passively or actively. The active linkages and joints have actuators through which their values can be controlled, whereas passive ones change their values to comply with the terrain topology.

The goal of kinematics modeling is to relate the motion of the rover body to the motions of the wheels. In order to achieve this we attach a sequence frames starting at the rover reference frame then the suspension joints, steering and finally the wheel-terrain contact frame. Let $u_i = [\, x_i \quad y_i \quad z_i \,]^T$ and $u_{i+1} = [\, x_{i+1} \quad y_{i+1} \quad z_{i+1} \,]^T$ denote the position of the current and next frames, respectively. Similarly, let $\varphi_i = [\, \alpha_i \quad \beta_i \quad \gamma_i \,]^T$ and $\varphi_i = [\, \alpha_i \quad \beta_i \quad \gamma_i \,]^T$ be the orientation of the current and next frames, respectively, where α, β and γ are the rotation around *x, y* and *z* axes, or roll, pitch and yaw, respectively. In the case of rovers, we are generally more interested in the translational and rotational velocities than position/orientation. The 3×1 translation velocity vector of the next frame *i+1* is dependent on the translational and rotational velocities of the current frame *i* plus any translational velocity added to the frame *i+1* itself. This can be written as [16]

$$\dot{u}_{i+1} = R_{i+1,i}\left(\dot{u}_i + \dot{\varphi}_i \times p_{i,i+1}\right) + \tilde{\dot{u}}_{i+1} \quad i = 1,2,\cdots,n-1 \tag{1}$$

where $R_{i+1,i}$ is the rotation matrix of the frame $i+1$ relative to the frame i, $p_{i,i+1}$ is the position vector of the origin of the coordinate frame i+1 expressed in coordinate frame i, and $\tilde{\dot{u}}_{i+1}$ is the translational velocity added to the frame $i+1$ due to the velocity of the frame i+1 itself. The latter is zero if the joint associated with the frame $i+1$ is not prismatic. The rotational velocity of the next frame $i+1$ is [16]

$$\dot{\varphi}_{i+1} = R_{i+1,i}\,\dot{\varphi}_i + \tilde{\dot{\varphi}}_{i+1} \qquad i = 1,2,\cdots,n-1 \tag{2}$$

Equation (2) shows that the rotational velocity of the frame $i+1$ is the sum of the effects of the rotational velocity of the frame i plus any rotational velocity $\tilde{\dot{\varphi}}_{i+1}$ added to the frame $i+1$. The latter is caused by the rotational joints associated with frame i+1. Equations (1)-(2) are not in a form that can be used in a straightforward manner. Our goal is to develop a universal method for using the Denavit-Hartenburg (D-H) parameters to model the frame to frame motion.

Using D-H notation, four parameters describe the transformation from frame i to frame $i+1$ given by rotation γ_i about z-axis, translation d_i along z-axis, translation a_i along x-axis, and rotation α_i about x-axis. Cascading these four transformations in the order just described, we obtain the transformation from frame i to frame $i+1$ as

$$T_{i,i+1} = \begin{bmatrix} c\gamma_i & -c\alpha_i s\gamma_i & s\alpha_i s\gamma_i & a_i c\gamma_i \\ s\gamma_i & c\alpha_i c\gamma_i & -s\alpha_i c\gamma_i & a_i s\gamma_i \\ 0 & s\alpha_i & c\alpha_i & d_i \\ 0 & 0 & 0 & 1 \end{bmatrix} \tag{3}$$

where c and s denote cosine and sine functions respectively. Using (3), we can extract the position vector $p_{i,i+1}$ needed in (1) as

$$p_{i,i+1} = \begin{bmatrix} a_i c\gamma_i \\ a_i s\gamma_i \\ d_i \end{bmatrix} \tag{4}$$

The transformation from frame $i+1$ to i is the inverse of the homogeneous transformation matrix (3) , i.e.

$$T_{i+1,i} = \begin{bmatrix} c\gamma_i & s\gamma_i & 0 & -a_i \\ -c\alpha_i s\gamma_i & c\alpha_i c\gamma_i & s\alpha_i & -d_i s\alpha_i \\ s\alpha_i s\gamma_i & -s\alpha_i c\gamma_i & c\alpha_i & -d_i c\alpha_i \\ 0 & 0 & 0 & 1 \end{bmatrix} \tag{5}$$

We extract the rotation $R_{i+1,i}$ from (5) as

$$R_{i+1,i} = \begin{bmatrix} c\gamma_i & s\gamma_i & 0 \\ -c\alpha_i s\gamma_i & c\alpha_i c\gamma_i & s\alpha_i \\ s\alpha_i s\gamma_i & -s\alpha_i c\gamma_i & c\alpha_i \end{bmatrix} \equiv R_i \tag{6}$$

In order to find the translational and rotational velocities $\tilde{\dot{u}}_{i+1}$ and $\tilde{\dot{\varphi}}_{i+1}$ added to the frame $i+1$ due to the motions of these frames, we consider the instantaneous transformation $T_{i+1,i+1}(t-\Delta t,t)$ that describes the transformation from the frame i+1 at time $(t-\Delta t)$ to this the same frame at time t. This matrix can be written as

$$T_{i+1,i+1}(t-\Delta t,t) = T_{i+1,i}\,(t-\Delta t,t-\Delta t)\,T_{i,i+1}(t-\Delta t,t) \tag{7}$$

Taking the derivative of (7), and considering that $T_{i+1,i}\,(t-\Delta t,t-\Delta t)$ is constant, we obtain

$$\dot{T}_{i+1,i+1}(t-\Delta t,t) = T_{i+1,i}\,(t-\Delta t,t-\Delta t)\,\dot{T}_{i,i+1}(t-\Delta t,t) \tag{8}$$

In order to express the above in terms of the D-H parameters, we take the derivative of (3) with respect to time, pre-multiply the result by (5) and substitute in (8) to obtain

$$\dot{T}_{i+1,i+1} = \begin{bmatrix} 0 & c\alpha_i\,\dot{\gamma}_i & s\alpha_i\,\dot{\gamma}_i & \dot{a}_i \\ c\alpha_i\,\dot{\gamma}_i & 0 & -\dot{\alpha}_i & s\alpha_i\,\dot{d}_i + a_i c\alpha_i\,\dot{\gamma}_i \\ -s\alpha_i\,\dot{\gamma}_i & \dot{\alpha}_i & 0 & c\alpha_i\,\dot{d}_i - a_i s\alpha_i\,\dot{\gamma}_i \\ 0 & 0 & 0 & 0 \end{bmatrix} \tag{9}$$

where the argument $(t-\Delta t,t)$ has been dropped to simplify the notation. It is noted that $\dot{T}_{i+1,i+1}$ can also be found for a general body in motion, which is given by [16]

$$\dot{T}_{i+1,i+1} = \begin{bmatrix} 0 & -\tilde{\dot{\varphi}}_z & \tilde{\dot{\varphi}}_y & \tilde{\dot{x}} \\ \tilde{\dot{\varphi}}_z & 0 & -\tilde{\dot{\varphi}}_x & \tilde{\dot{y}} \\ -\tilde{\dot{\varphi}}_y & \tilde{\dot{\varphi}}_x & 0 & \tilde{\dot{z}} \\ 0 & 0 & 0 & 0 \end{bmatrix} \tag{10}$$

where $\tilde{\dot{x}}$, $\tilde{\dot{y}}$, $\tilde{\dot{z}}$ are the components of $\tilde{\dot{u}}_{i+1}$, and $\tilde{\dot{\varphi}}_x$, $\tilde{\dot{\varphi}}_y$ and $\tilde{\dot{\varphi}}_z$ are the components of $\tilde{\dot{\varphi}}_{i+1}$. Equating the like terms in (9) and (10), we have

$$\tilde{u}_{i+1} = \begin{bmatrix} \dot{a}_i \\ s\alpha_i\,\dot{d}_i + a_i c\alpha_i\ \dot{\gamma}_i \\ c\alpha_i\,\dot{d}_i - a_i s\alpha_i\ \dot{\gamma}_i \end{bmatrix} = \begin{bmatrix} 0 & 0 & 1 & 0 \\ a_i c\alpha_i & s\alpha_i & 0 & 0 \\ -a_i s\alpha & c\alpha_i & 0 & 0 \end{bmatrix} \begin{bmatrix} \dot{\gamma}_i \\ \dot{d}_i \\ \dot{a}_i \\ \dot{\alpha}_i \end{bmatrix} \equiv A_i \dot{\eta}_i \tag{11}$$

$$\tilde{\varphi}_{i+1} = \begin{bmatrix} \dot{\alpha}_i \\ s\alpha_i\ \dot{\gamma}_i \\ c\alpha_i\ \dot{\gamma}_i \end{bmatrix} = \begin{bmatrix} 0 & 0 & 0 & 1 \\ s\alpha_i & 0 & 0 & 0 \\ c\alpha_i & 0 & 0 & 0 \end{bmatrix} \begin{bmatrix} \dot{\gamma}_i \\ \dot{d}_i \\ \dot{a}_i \\ \dot{\alpha}_i \end{bmatrix} \equiv B_i \dot{\eta}_i \tag{12}$$

where η_i is the D-H parameter vector, and A_i and B_i are sparse 3×4 coefficient matrices. It is seen from (11) and (12) that $\tilde{u}_{i+1}$ and $\tilde{\varphi}_{i+1}$ are linear in the derivative of the D-H parameter vector $\dot{\eta}_i$. There is one more substitution needed before we express the final results. We note that the cross product term in (1) can be expressed as

$$\dot{\varphi}_i \times p_{i+1} = \dot{\varphi}_i \times \begin{bmatrix} -a_i \\ -d_i\ s\alpha_i \\ -d_i c\alpha_i \end{bmatrix} = -S_i \dot{\varphi}_i \tag{13}$$

where

$$S_i = \begin{bmatrix} 0 & d_i c\alpha_i & -d_i s\alpha_i \\ -d_i c\alpha_i & 0 & a_i \\ d_i s\alpha_i & -a_i & 0 \end{bmatrix} \tag{14}$$

and S_i is a skew symmetric matrix. Finally, the equations of velocity propagation (1)-(2) can now be expressed as

$$\begin{bmatrix} \dot{u}_{i+1} \\ \dot{\varphi}_{i+1} \end{bmatrix} = \begin{bmatrix} R_i & -R_i S_i \\ 0 & R_i \end{bmatrix} \begin{bmatrix} \dot{u}_i \\ \dot{\varphi}_i \end{bmatrix} + \begin{bmatrix} A_i \\ B_i \end{bmatrix} \dot{\eta}_i \tag{15}$$

where R_i, S_i, A_i and B_i are given by, respectively by (6), (14), (11) and (12). Equation (15) expresses the position and orientation rates (configuration rate) of the next frame $i+1$ in terms of the rates of the current frame i. The coefficient matrices R_i, S_i, A_i and B_i are dependent only on the D-H parameters. The D-H parameter table can readily be set up from the rover link-joint arrangements, as demonstrated in the following section. It is also interesting to note that the D-H parameter derivatives $\dot{\eta}$ affect linearly the velocities of the next frame. The above equation can be used to relate the position and orientation velocities of two frames in the chain $\{1,2,\cdots,n_{j-1}\}$ where 1 refers to the rover reference frame, n_{j-1} is a wheel axel frame, $j=1,2,\cdots,w$ and w is the number of wheels.

We must define one more frame, i.e. the contact frame C_j where the motion over the terrain takes place. This frame is numbered n_j in the chain. Since the transformation from the axel frame A_j to the contact frame is the same for any wheeled rover, we derive this transformation explicitly. The contact frame C_j is shown in Fig. 1 where its *x*-axis is tangent to the terrain at the point of contact and its *z*-axis is normal to the terrain. The contact angle, denoted by δ_j, is the angle between the *z*-axes of the *j*-th wheel axel and the contact coordinate frames, as shown in Fig. 1. The contact frame is obtained from the axel frame by rotating δ_j about the axel , then translating by the wheel radius *r* in the negative *z* direction. Thus the rotation matrix to be used in (15) is

$$R_{n_j} = \begin{bmatrix} c\delta_j & 0 & s\delta_j \\ 0 & 1 & 0 \\ -s\delta_j & 0 & c\delta_j \end{bmatrix} \tag{16}$$

The position vector p_{n_j+1} for the this last frame, and its corresponding skew symmetric matrix to be used in (15) are

$$p_{n_j} = \begin{bmatrix} -r\,s\delta_j \\ 0 \\ -r\,c\delta_j \end{bmatrix}; \quad S_{n_j} = \begin{bmatrix} 0 & r\,c\delta_j & 0 \\ -r\,c\delta_j & 0 & r\,s\delta_j \\ 0 & -r\,s\delta_j & 0 \end{bmatrix} \tag{17}$$

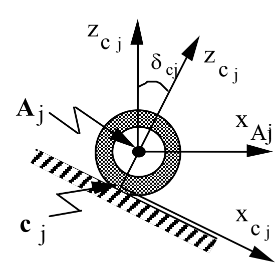

Fig. 1 Definition of contact angle

The vector $\dot{\eta}_i$ for the contact frame to be used in (15) consists of the wheel angle rolling rate $\dot{\theta}_j$, which causes the linear motion $r\dot{\theta}_j$ along *x*-axis of the terrain, as well as various wheel slips rates. In the most general case, there will be six slips rates - three affecting velocities along $\dot{x}, \dot{y}, \dot{z}$ and three affecting the orientation angles $\dot{\alpha}, \dot{\beta}, \dot{\gamma}$. The first three slip rates are roll, side and bounce (up and down off the terrain movement) denoted by $\dot{\zeta}_{roll,j}$, $\dot{\zeta}_{side,j}$ and $\dot{\zeta}_{bnce,j}$. The second three are slip rates are tilt, sway and turn denoted by $\dot{\zeta}_{tilt,j}$, $\dot{\zeta}_{sway,j}$, $\dot{\zeta}_{turn,j}$. However, including all six slips at each wheel provides too many degrees of freedom making the motion erratic and unpredictable. In addition the roll slip rate $\dot{\zeta}_{roll,j}$ cannot be distinguished from wheel roll rate $r\dot{\theta}_j$, bounce $\dot{\zeta}_{bnce,j}$ cannot be considered without including dynamic effects, and sway is usually prevented because of the mechanical design. For these reasons we consider only three of the slip rates in the kinematics model here and thus the second term on the right side of (15) for the contact frame is

$$\begin{bmatrix} A_{n_j} \\ B_{n_j} \end{bmatrix} \dot{\eta}_{n_j} = \begin{bmatrix} r & 0 & 0 & 0 \\ 0 & 1 & 0 & 0 \\ 0 & 0 & 0 & 0 \\ 0 & 0 & 0 & 1 \\ 0 & 0 & 0 & 0 \\ 0 & 0 & 1 & 0 \end{bmatrix} \begin{bmatrix} \dot{\theta}_i \\ \dot{\zeta}_{side,j} \\ \dot{\zeta}_{turn,j} \\ \dot{\zeta}_{tilt,j} \end{bmatrix} \qquad (18)$$

The transformations (15) can be cascaded from the frame 1 to the frame n_j to obtain the equation of the motion of the rover reference frame in terms of the motion of a wheel contact frame, which will be of the form

$$\begin{bmatrix} \dot{u}_R \\ \dot{\varphi}_R \end{bmatrix} = E_j \begin{bmatrix} \dot{u}_{C_j} \\ \dot{\varphi}_{C_j} \end{bmatrix} + F_j \dot{\Gamma}_j \qquad j = 1,2,\cdots,w \qquad (19)$$

where E_j and F_j are coefficient matrices obtained by the cascading of the matrices in (15), and $\dot{\Gamma}_j = \begin{bmatrix} \dot{\eta}_1^T & \dot{\eta}_2^T & \cdots & \dot{\eta}_{n_j}^T \end{bmatrix}^T$ is the combined parameters rates. Equation (20) describes the contribution of individual wheel motion and the connecting joints and linkages to the rover body motion. The net body motion is the composite effect of all wheels and can be obtained by combining (19) into a single matrix equation as

$$\begin{bmatrix} I_6 \\ \vdots \\ I_6 \end{bmatrix} \begin{bmatrix} \dot{u}_R \\ \dot{\varphi}_R \end{bmatrix} = E \begin{bmatrix} \dot{u}_C \\ \dot{\varphi}_C \end{bmatrix} + F\dot{\Gamma} \qquad (20)$$

where the matrices E and F are the aggregate matrices obtained from E_j and F_j, $\dot{u}_C = \begin{bmatrix} \dot{u}_{C_1} & \cdots & \dot{u}_{C_w} \end{bmatrix}^T$ and $\dot{\varphi}_C = \begin{bmatrix} \dot{\varphi}_{C_1} & \cdots & \dot{\varphi}_{C_w} \end{bmatrix}^T$ respectively, and $\dot{\Gamma}$ is the vector of aggregate parameter rates. It is to be noted that (15), (19) and (20) can be developed for a given rover either analytically, e.g. using a symbolic software tool such as Matlab, or numerically. This kinematics model can be used for various applications, i.e. navigation, actuation of wheels, steering and active joints; slip detection, etc. In the following section we apply the method to an articulated rover.

III. Example

The high mobility rover to be considered here is similar to the JPL Sample Return Rover [14], and has an active suspension system. The schematic diagram of the rover to be modeled is shown in Fig. 2. The rover has four wheels with each independently actuated, and their rotation angles subscripted with a clockwise direction so that θ_1, θ_4 are for the left side and θ_2, θ_3 are for the right side. At either side of the rover, two legs are connected via an adjustable hip joint. In Fig. 2 the hip angle on the left and right sides is denoted by $2\sigma_1$, and the hip angle on the right side is $2\sigma_2$. These joints are actuated and used for balancing (leveling) the rover when traversing on an inclined surface. The two hips are connected to the body via a differential which has an angle ρ on the left side and $-\rho$ on the right side. On a flat surface ρ is zero but becomes non-zero when one side moves up or down with respect to the other side. The differential joint ρ is passive (unactuated) and provides for the compliance with the terrain. All four wheels are steerable with steering angles denoted by ψ_j, $j = 1,2,3,4$. The wheel terrain contact angles are δ_j, $j = 1,2,3,4$ as shown in Fig. 1.

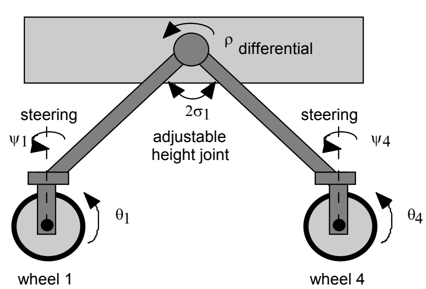

Fig. 2 Schematic diagram of the rover left side.

In order to derive the kinematics equations, we must assign coordinates frames. Fig. 3 illustrates our choice of coordinate frames for the left side of the rover. The right side is assigned similar frames. In Fig. 3, R is the rover reference frame whose origin is located on the center of gravity of the rover, its *x*-axis along the rover straight line forward motion, its y-axis across the rover body and its z-axis represents the up and down motion. The differential frame D has a vertical (along *z*-axis) offset denoted by k_1 and a horizontal distance of k_2 from D. The distance from the differential to the hip, denoted by k_3, is half the width of the rover. The length of the legs from the hip to the wheel axle is k_4. From the differential frame four chains branch off, each consists of a hip, a steering column and a wheel axel. The four frames for the hip, steering and axel are denoted, respectively, by $H_1,\cdots,H_4$; $S_1,\cdots,S_4$ and $A_1,\cdots,A_4$. Each frame is obtained from the previous frame in the chain by rotations and translations as shown with the D-H parameters $\gamma_i, d_i, a_i, \alpha_i$ in Table 1 and in Fig 3. Note that there are only two hip joints and thus $\sigma_4 = \sigma_1$ and $\sigma_3 = \sigma_2$. Fig. 4 shows the angle between the hip and steering frames, and between steering and axel frames for wheel 1.

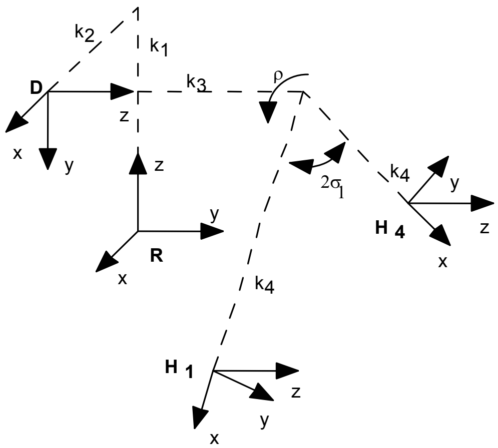

Fig. 3 Reference R, differential D, and hip H coordinate frames.

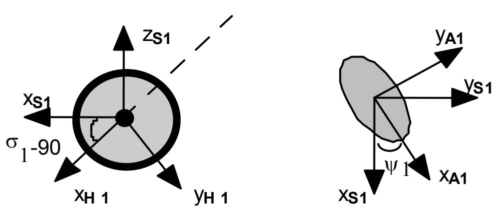

Fig. 4 Side view (left figure) and top view of wheel 1.

TABLE 1- D-H Parameters for the ARAS

Frame	γ_i	d_i	a_i	α_i	$\dot{\gamma}_i$
D	0	k_1	k_2	-90	0
H1	$90-\sigma_1+\rho$	k_3	k_4	0	$-\dot{\sigma}_1+\dot{\rho}$
H2	$90-\sigma_2-\rho$	$-k_3$	k_4	0	$-\dot{\sigma}_2-\dot{\rho}$
H3	$90+\sigma_3-\rho$	$-k_3$	k_4	0	$\dot{\sigma}_3-\dot{\rho}$
H4	$90+\sigma_4+\rho$	k_3	k_4	0	$\dot{\sigma}_4+\dot{\rho}$
S1	σ_1-90	0	0	90	$\dot{\sigma}_1$
S2	σ_2-90	0	0	90	$\dot{\sigma}_2$
S3	σ_3-90	0	0	90	$\dot{\sigma}_3$
S4	σ_4-90	0	0	90	$\dot{\sigma}_4$
A1	ψ_1	0	0	0	$\dot{\psi}_1$
A2	ψ_2	0	0	0	$\dot{\psi}_2$
A3	ψ_3	0	0	0	$\dot{\psi}_3$
A4	ψ_4	0	0	0	$\dot{\psi}_4$

We now use the basic frame to frame equation (16) and go through the frames sequentially starting with the rover reference R and going to differential D, a hip H_j, a steering S_j, a wheel axel A_j and finally to a wheel contact C_j frame.

The transformation from the rover reference *R* (frame *i=1*) to the differential (frame *i=2*) is constant translational only, and thus no D-H parameter derivative is involved. Substituting the values of the D frame from Table 1, i.e. $\gamma_1 = 0$, $d_1 = k_1, a_1 = k_2$, $\alpha_1 = 90^o$, into (16) with R_1, S_1, A_1 and B_1 given, respectively, by (6), (14), (11) and (12), we get

$$\begin{bmatrix}\dot{u}_D \\ \dot{\varphi}_D\end{bmatrix} = \begin{bmatrix} 1 & 0 & 0 & 0 & -k_1 & 0 \\ 0 & 0 & -1 & 0 & -k_2 & 0 \\ 0 & 1 & 0 & k_1 & 0 & -k_2 \\ 0 & 0 & 0 & 1 & 0 & 0 \\ 0 & 0 & 0 & 0 & 0 & -1 \\ 0 & 0 & 0 & 0 & 1 & 0 \end{bmatrix} \begin{bmatrix}\dot{u}_R \\ \dot{\varphi}_R\end{bmatrix} \tag{21}$$

Next in the chain is a hip frames. Using Table 1 and (15) we obtain the following equation which applies to all four hip frames indexed by *j*.

$$\begin{bmatrix}\dot{u}_{Hj} \\ \dot{\varphi}_{Hj}\end{bmatrix} = \begin{bmatrix} -s\lambda_j & c\lambda_j & 0 & b_j k_3 c\lambda_j & b_j k_3 s\lambda_j & 0 \\ -c\lambda_j & -s\lambda_j & 0 & -b_j k_3 s\lambda_j & b_i k_3 c\lambda_j & -k_4 \\ 0 & 0 & 1 & k_4 c\lambda_j & -k_4 s\lambda_j & 0 \\ 0 & 0 & 0 & -s\lambda_j & c\lambda_j & 0 \\ 0 & 0 & 0 & -c\lambda_j & -s\lambda_j & 0 \\ 0 & 0 & 0 & 0 & 0 & 1 \end{bmatrix} \begin{bmatrix}\dot{u}_D \\ \dot{\varphi}_D\end{bmatrix}$$
$$+ \begin{bmatrix}0 & k_4 & 0 & 0 & 0 & 1\end{bmatrix}^T \left(\dot{\sigma}_j + b_j \dot{\rho}\right); \quad j = 1,2,3,4 \tag{22}$$

where $\lambda_j = h_j \sigma_j + b_j \rho$, $h_j = \begin{cases} -1 & j = 1,2 \\ +1 & j = 3,4 \end{cases}$, and $b_j = \begin{cases} +1 & j = 1,4 \\ -1 & j = 2,3 \end{cases}$. Note that (22) has a D-H parameter rate component which due to the motion of the differential and hip joint angles. We now proceed to the steering frame, and use (15) and the steering row of Table 1 to obtain

$$\begin{bmatrix}\dot{u}_{Sj} \\ \dot{\varphi}_{Sj}\end{bmatrix} = \begin{bmatrix} s\sigma_j & -c\sigma_j & 0 & 0 & 0 & 0 \\ 0 & 0 & 1 & 0 & 0 & 0 \\ -c\sigma_j & -s\sigma_j & 0 & 0 & 0 & 0 \\ 0 & 0 & 0 & s\sigma_j & -c\sigma_j & 0 \\ 0 & 0 & 0 & 0 & 0 & 1 \\ 0 & 0 & 0 & -c\sigma_j & -s\sigma_j & 0 \end{bmatrix} \begin{bmatrix}\dot{u}_{Hj} \\ \dot{\varphi}_{Hj}\end{bmatrix} + \begin{bmatrix}0 \\ 0 \\ 0 \\ 0 \\ 1 \\ 0\end{bmatrix} \dot{\sigma}_j$$
$$j = 1,2,3,4 \tag{23}$$

Similarly the transformation from the steering frame to the axel frame is found as

$$\begin{bmatrix} \dot{u}_{Aj} \\ \dot{\varphi}_{Aj} \end{bmatrix} = \begin{bmatrix} c\psi_j & s\psi_j & 0 & 0 & 0 & 0 \\ -s\psi_j & c\psi_j & 0 & 0 & 0 & 0 \\ 0 & 0 & 1 & 0 & 0 & 0 \\ 0 & 0 & 0 & c\psi_j & s\psi_j & 0 \\ 0 & 0 & 0 & -s\psi_j & c\psi_j & 0 \\ 0 & 0 & 0 & 0 & 0 & 1 \end{bmatrix} \begin{bmatrix} \dot{u}_{Sj} \\ \dot{\varphi}_{Sj} \end{bmatrix} + \begin{bmatrix} 0 \\ 0 \\ 0 \\ 0 \\ 0 \\ 1 \end{bmatrix} \dot{\psi}_j$$

$$j = 1,2,3,4 \qquad (24)$$

Finally, the axel to the contact frame transformation matrices are given by (15)-(18), i.e.

$$\begin{bmatrix} \dot{u}_{Cj} \\ \dot{\varphi}_{Cj} \end{bmatrix} = \begin{bmatrix} c\delta_j & 0 & s\delta_j & 0 & r & 0 \\ 0 & 1 & 0 & -rc\delta_j & 0 & -rs\delta_j \\ -s\delta_j & 0 & c\delta_j & 0 & 0 & 0 \\ 0 & 0 & 0 & c\delta_j & 0 & s\delta_j \\ 0 & 0 & 0 & 0 & 1 & 0 \\ 0 & 0 & 0 & -s\delta_j & 0 & c\delta_j \end{bmatrix} \begin{bmatrix} \dot{u}_{Aj} \\ \dot{\varphi}_{Aj} \end{bmatrix}$$

$$+ \begin{bmatrix} r & 0 & 0 & 0 \\ 0 & 1 & 0 & 0 \\ 0 & 0 & 0 & 0 \\ 0 & 0 & 0 & 1 \\ 0 & 0 & 0 & 0 \\ 0 & 0 & 1 & 0 \end{bmatrix} \begin{bmatrix} \dot{\theta}_i \\ \dot{\zeta}_{side,j} \\ \dot{\zeta}_{turn,j} \\ \dot{\zeta}_{tilt,j} \end{bmatrix} \qquad (25)$$

Equations (21)-(25) can be combined to form the composite equations (19)-(20). It is noted that most matrices in (21)-(25) are sparse.

IV. CONCLUSIONS

A new methodology is presented for the kinematics modeling of high mobility rovers. The approach is very general and can be applied to any wheeled rover and only requires setting up the D-H table for the rover links and joints. The main feature of the work is its generality, e.g. dealing with both active (actuated) and passive joints and linkages, and its ease of implementation. In particular, the proposed formulation makes the computer implementation very efficient through simple repeated function calls. We have developed a computer program that reads the D-H table of a rover, and generates the equations of the rover motion symbolically, or computes various coefficient matrices of the rover motion numerically. The latter can be used for real-time control of rovers.

REFERENCES

[1] Schenker, P., T. Huntsberger, P. Pirjanian, E. Baumgartner, and E. Tunstel, " Planetary rover developments supporting Mars exploration, sample return and future human robotic colonization", *Autonomous Robots*, vol. 14, pp. 103-126, 2003.

[2] Volpe, R., "Rover functional autonomy development for Mars mobile science", *Proc. IEEE Aerospace Conf.* pp. 643-652, 2003.

[3] Gonthier, Y., and E. Papadopoulos, "On the development of a real-time simulator for and electro-hydraulic forestry machine", *Proc. IEEE Int. Conf. Robotics & Automation,* Leuven, Belgium, 1988.

[4] Baerveldt,A-J. Ed., "Agricultural Robotics", Autonomous Robots, Vol 13-1, Kluwer Academic Publishers, 2002.

[5] Cunningham, J., J. Roberts, P. Corke and H. Durrant-Whyte, "Automation of underground LHD and truck haulage", Proc. Australian IMM Conf.. pp. 241-246, 1998.

[6] DeBolt, Ch., Ch. O'Donnell, S. Freed, and T. Nguyen, "The bugs 'basic uxo gathering system' project for uxo clearance and mine countermeasures", *Proc. IEEE Int. Conf. Robotics and Automation, pp. 329-334, Albuquerque, N.M., 1997.*

[7] Sreenivasan, S. and K. Waldron, "Displacement analysis of an actively articulated vehicle configuration with extensions to motion planning on uneven terrain", *Trans. ASME J. Mechanical Design*, vol. 118, pp. 312-317, 1966.

[8] Iagnemma, K. and S. Dubowski, " Traction Control of wheel mobile robots in rough terrain with applications to planetary rovers," *Int. J. Robotics Res*., vol. 23, No. 10-11, pp. 1029-1040, 2003.

[9] P.F. Muir and C.P. Neumann, "Kinematic modeling of wheeled mobile robots," J. Robotic Systems, vol. 4, no. 2, pp. 282-340, 1987.

[10] G. Campion, G. Bastin and diAndrea-Novel, "Structural properties and classification of kinematic and dynamic models for wheel mobile robots," IEEE Trans. Robotics and Automation, Vol. 12, No. 1, Feb. 1996.

[11] B.J. Choi and S.V. Sreenivasan, "Gross motion characteristics of articulated mobile robots with pure rolling capability on smooth uneven surfaces," IEEE Trans. Robotics and Automation, Vol. 15, No. 2, pp. 340-343, 1999.

[12] M. Tarokh, G. McDermott, S. Hayati, and J. Hung, "Kinematic modeling of a high mobility Mars rover," Proc. IEEE Int. Conf. Robotics and Automation, pp. 992-998, Detroit, MI, 1999.

[13] K. Iagnemma and S. Dubowski, "Vehicle-ground contact angle estimation with application to mobile robot traction," Proc. 7th Int. Conf. on Advances on Robot Kinematics, Ark '00, pp. 137-146, 2000.

[14] J. Balaram, "Kinematic observers for articulated rovers,", Proc. IEEE Int. Conference on Robotics and Automation, pp. 2597-2604, San Francisco, CA, 2000.

[15] Tarokh, M. and G. McDermott, " Kinematics Modeling and Analysis of Articulated Rovers", *IEEE Trans. Robotics*, vol. 21, No. 4, 539-553, 2005.

[16] Craig, J. Introduction to Robotics, Mechanics and Control, pp.144-146, Pearson Prentice-Hall, 2005.